

A High-Lateral Resolution MALDI Microprobe Imaging Mass Spectrometer Utilizing an Aspherical Singlet Lens

Sang Yun Han,* Hwan Jin Kim, and Tae Kyung Ha

Center for Nano-Bio Convergence, Korea Research Institute of Standards and Science, Daejeon 305-340, Korea

*E-mail: sanghan@kriss.re.kr

Received September 24, 2012, Accepted October 31, 2012

We report the construction of a MALDI imaging mass spectrometer equipped with a specially designed laser focusing lens, a compact aspherical singlet lens, that obtains a high-lateral imaging resolution in the microprobe mode. The lens is specially designed to focus the ionization laser ($\lambda = 355$ nm) down to a 1 μm diameter with a long working distance of 34.5 mm. With the lens being perpendicular to the sample surface and sharing the optical axis with the ion path, the imaging mass spectrometer achieved an imaging resolution of as good as 5 μm along with a high detection sensitivity of 100 fmol for peptides. The mass resolution was about 900 ($m/\Delta m$) in the linear TOF mode. The high-resolution capability of this instrument will provide a new research opportunity for label-free imaging studies of various samples including tissues and biochips, even for the study at a single cell level in the future.

Key Words : Imaging mass spectrometry, High-lateral resolution, MALDI

Introduction

Due to its promising potential for bioclinical applications, including biomarker discovery and disease diagnosis, matrix-assisted laser desorption/ionization (MALDI) mass spectrometric imaging has been being actively developed in recent years.^{1,2} It opens a unique opportunity often referred to as biochemical mapping, providing images carrying high-content biomolecular information without the necessity of labeling target molecules. In the development, various technical issues have been carefully investigated: matrix treatment methods as well as matrices for more sensitive and reliable ionization from the sample surfaces;³⁻⁶ the method of on-tissue/on-chip tryptic digestion for characterization of protein peaks observed in the mass images;⁷⁻⁹ data processing and statistical analysis of image data to elucidate bioclinical significance^{10,11} and the like. By virtue of such concerted efforts, significant progress has been recently witnessed in the emerging field of MALDI mass spectrometric imaging, which is beginning to find its applications of which an example is cancer diagnosis by tissue imaging in the real clinical field.¹²

On the other hand, the development of new high-lateral resolution imaging instruments is another important area to extend the capability of mass spectrometric imaging, even to a single cell level. Currently, mass spectrometric imaging heavily relies on commercial MALDI-TOF (time-of-flight) mass spectrometers. However, due to the nature of the conventional MALDI-TOF design, more specifically, the well-established two-stage acceleration scheme to achieve the best mass resolution from a TOF instrument,¹³ focusing the laser that determines the image resolution has been limited. Thus, the routine image resolution in the so-called microprobe mode with commercial MALDI-TOF mass spectro-

eters has been only about 100 μm , no better than a few tens of micrometers. In this regard, the MALDI-TOF mass spectrometers dedicated to mass spectrometric imaging were developed and offered a spatial imaging resolution of higher than 10 μm .^{14,15} The imaging instruments were featured by a specially designed laser focusing optics, a multicomponent UV objective lens with a bore along the optical axis. The objective lens was combined with the ionization and the extraction/acceleration region, of which bore offered a path for ions produced in the source to fly into the TOF mass analyzer. Since that accomplishment, the multicomponent objective lens system has been widely utilized on various mass spectrometric platforms, including FT-ICR and Orbitrap to exploit high resolution both in space and the mass spectrum.^{16,17} As an alternative to the method of laser micro-focusing and stage scanning, the new imaging scheme based on the time and position-sensitive detector is also currently being developed and is known as the microscope mode.¹⁸ However, the performance of the detector still needs further improvement¹⁹ in order to meet the need for simultaneous characterization and localization of various biomolecules in the mass images.

In this work, we report the construction of a high-spatial resolution MALDI imaging mass spectrometer operated in the microprobe mode, which employs a compact, aspherical singlet laser focusing lens that replaces the previous bulky assembly of the multicomponent objective lens system.

Experimental

Materials. For standard peptides, a peptide kit was obtained from Bruker Bioscience. The kit contained bradykinin 1-7 (monoisotopic mass = 747.4 Da), angiotensin II (1046.5 Da), substance P (1347.7 Da), bombesin (1619.8 Da), renin

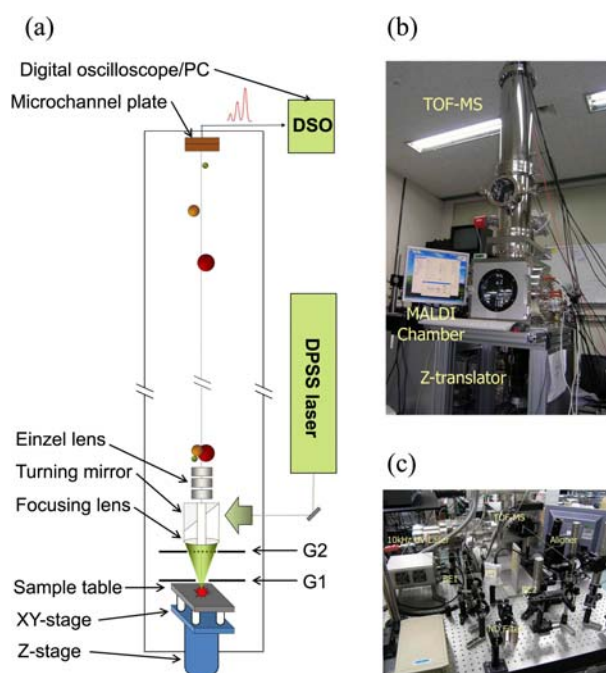


Figure 1. (a) Schematic diagram and (b) picture for the MALDI imaging mass spectrometer, (c) picture for the laser and optics setting.

substrate (1758.9 Da), ACTH 1-17 (2093.1 Da), and ACTH 18-39 (2465.2 Da). 2,5-DHB (dihydroxybenzoic acid) and α -CHCA (α -cyano-4-hydroxycinnamic acid) were purchased from Sigma-Aldrich Korea, which were employed as matrices. The reagents were used without further purification.

Construction of a MALDI Imaging Mass Spectrometer.

Figure 1 displays the schematic diagram of the lab-built MALDI imaging mass spectrometer. The imaging mass spectrometer consists of two vacuum chambers. One is the MALDI chamber that contains a laser focusing lens assembly, the extraction aperture (G1) and acceleration grid (G2) electrodes, an einzel lens, a pair of deflector plates, and the table for the MALDI plate sitting on the XY-Z translational stage. The other chamber houses a TOF mass spectrometer, which has a TOF/TOF functionality²⁰ equipped with a reflectron but was mainly used in linear mode for imaging mass spectrometry. The two chambers were separated by a vacuum gate valve and pumped independently by two turbo pumps, so that the vacuum in the TOF mass spectrometer side was maintained during maintenance of the ionization chamber, including the sample change. The typical working pressure during the MALDI experiments was 8×10^{-8} torr. Although special vibration damping system was not employed, vibrations from floors, mechanical pumps, and turbo pumps were carefully isolated by properly using materials such as long flexible pumping lines and thick industrial damping rubbers.

The XY-Z translational stage consists of a commercial XY stage (MT84-50-LM-XY-UHV; repeatability = 0.8 μ m; travel distance = 50 mm; Feinmess Dresden, GmbH) located in the ionization chamber and an additional lab-built heavy-duty Z stage attached on the bottom of chamber outside vacuum,

which the XY stage mounted. Because of the large replacement provided by the XY stage, the mass spectrometer can use large-format commercial MALDI plates. The sample table was placed on top of the XY stage, where it was electrically isolated from the stage with 2"-long ceramic standoffs. Being equipped with a precision feed-back strip encoder system with a 50-nm step resolution (RGH22; RENISHAW, Inc.), the Z stage was capable of precisely determining the height of the sample table. In fact, it was a crucial function offering a fine adjustment of laser focusing on the sample surfaces.

The lens assembly consisting of a singlet, aspherical plano-convex lens and a turning mirror was custom-built by Korea Electro-Optics, Inc. The lens design was carried out using the Zemax program (Radiant Zemax). The simulation results are electronically available in the Supporting information. The lens was made of an optical material with a refractive index (n at 355 nm) of 1.6249. By employing an aspherical system with an entrance pupil diameter of 35 mm, we achieved a high numerical aperture of 0.40 with a long working distance of 34.5 mm, which were well suited to the given geometrical constraints. The simulated optical, Airy radius of the lens was 0.495 μ m, which indicated the focusing capability of a 355 nm laser beam to a micrometer level. The calculated encircled energy also showed that about 75% of the incident laser energy would be focused into a circle with a diameter of 1 μ m, which is the diameter that may be the most relevant to the MALDI process. In the assembly, the turning mirror was attached right behind the lens, which steered the incoming laser beam down to the lens. The lens assembly as a whole was located at the entrance of the TOF mass analyzer after the ion source region, immediately followed by an einzel lens and a set of deflectors. It possessed a bore along the optical axis, in which a stainless steel tube with a 6 mm inner diameter was placed. The tube offered the pathway for produced ions to fly into the TOF mass analyzer through the lens assembly. For MALDI, a Q-switched DPSS (diode-pumped solid state) laser ($\lambda = 355$ nm) with a maximum repetition rate of 10 kHz was used (UVFQ-100-1-Y-355; Elforlight, Ltd.). The laser power was controlled using ND filters (CVI), and the laser beam was expanded and parallelized to about 40 mm in diameter using two lab-built beam expanders. To ensure that the expanded beam shines on the lens surface at the correct angle, we devised and implemented an interferometric device.

The ion optics used in this imaging mass spectrometer was carefully designed using the SIMION simulation program (Scientific Instrument Services, Inc). The optimized distance between the sample and the extraction aperture (G1) was 4 mm, and the separation between the extraction (G1) and acceleration (G2) electrodes was 18 mm. The acceleration electrode was a grid plate, which was placed in front of the lens assembly. However, the extraction plate had to have an aperture of 4.5 mm in diameter so that the focused beam could irradiate the sample surface without being blurred by a grid. In fact, this small aperture created a certain focusing effect on MALDI ions just produced from the sample surface.

The effect was simulated to be rather strong, tightly focusing ions at the entrance of the lens assembly. Due to this effect, the einzel lens located behind the lens assembly played an important role, which parallelized and guided diverging ions to the TOF microchannel plate detector. Typically, 20-keV ion kinetic energy was used, and the voltage pulses generated by a commercial pulser (GRX; DEI, Inc.) extracted ions into the acceleration region in the ion source. The mass spectra were recorded at the end of a TOF flight tube using a dual MCP assembly (Burle Electro-Optics, Inc.), for which signals were averaged and stored using a digital oscilloscope (DPO 7254; Tektronix). All pulsed events including delayed extraction were synchronized in time using delay generators with a picosecond resolution (DG 535; SRS, Inc.).

Data and Results

Mass Spectrum. First, we optimized the imaging instrument for mass spectrometry in the linear mode that offered a good ion transmission; thus, it had a higher sensitivity than in the reflectron mode. It also possessed a theoretically unlimited mass range. Due to such merits, the linear TOF mode has been the conventional choice of mass spectrometric imaging for biological samples such as tissues. The optimization was performed using a peptide kit that expanded the mass range from 700 Da to 2500 Da, which is suitable for proteomics research. In the optimization, it was learned that the laser alignment was critical in this ion source geometry, as it is probably related to the fact that where to hit on the sample surface influences guiding the generated MALDI ions properly through the lens assembly into the TOF mass spectrometer. Thereby, the optimum condition for mass spectrometry was found at the laser alignment where the best spatial resolution was also achieved. An example of the resulting MALDI mass spectrum is given in Figure 2, which was obtained using a 355 nm DPSS laser with a 10 $\mu\text{J}/\text{pulse}$ energy (20 Hz). In the experiment, the sample was prepared by the dried droplet method using a 2,5-DHB matrix on a stainless steel MALDI plate. As shown in the

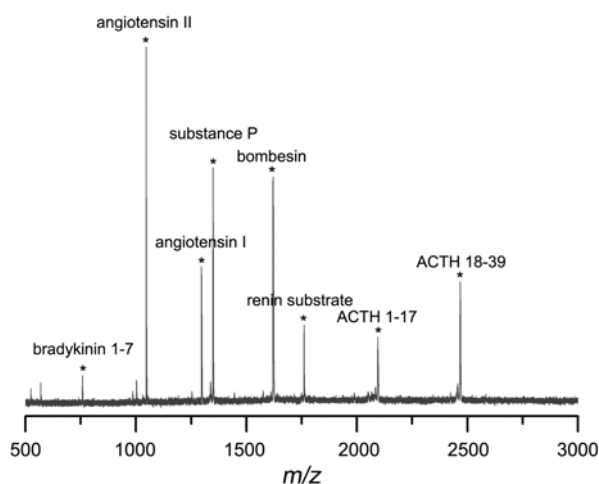


Figure 2. MALDI mass spectrum of a peptide mixture obtained using the imaging mass spectrometer in linear mode.

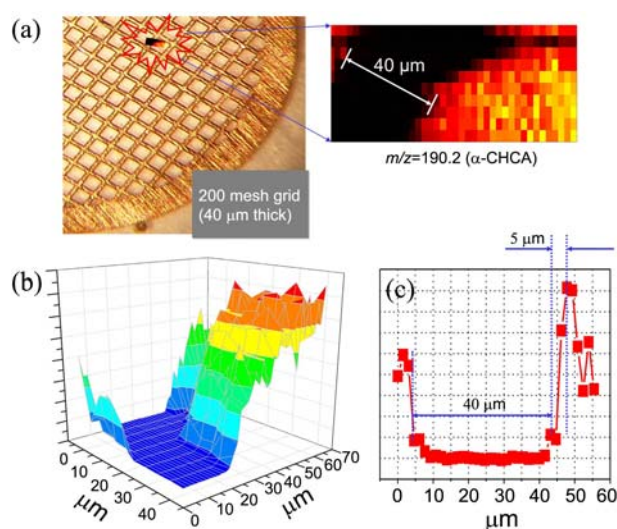


Figure 3. (a) Picture for the TEM grid and the mass image for patterned α -CHCA matrix obtained at $m/z = 190.2$ Da, (b) the 3D-view of the mass image, (c) the cross-sectional view of (b) shows the actual imaging resolution to be about 5 μm .

spectrum, the developed imaging mass spectrometer successfully recorded the test peptides with a mass resolution of about 900 in $m/\Delta m$, displaying a rather even mass resolution over the examined mass range. The mass spectrometer could detect 100 fmol angiotensin II, which exhibits the good detection sensitivity that this lab-built mass spectrometer provides.

Mass Spectrometric Imaging. To evaluate the imaging capability, we used a TEM grid with a known dimension, a 200 mesh grid (125 μm pitch) with a 40 μm thickness. A thin film of matrix (α -CHCA) was deposited on the stainless steel MALDI plate. The TEM grid was placed by being gently pressed on the matrix layer. This obtained the patterned matrix film, with dimensions defined by the TEM grid. With respect to the test sample, mass spectrometric imaging was conducted by the stage scan with a 1 μm grid step using the XY stage. Using the Z stage, the distance between the sample surface and the focusing lens was carefully adjusted, which determined the laser focusing on the sample surface. Typically, the Z stage was examined with a 1 μm step.

A representative mass image is given in Figure 3. The image was taken crossing a single grid line with a thickness of 40 μm , where MALDI ions could not be generated due to the presence of the grid mask. As demonstrated in the mass image for α -CHCA ions ($m/z = 190.2$ Da), the newly constructed imaging mass spectrometer clearly provides a high-lateral resolution mass image. As analyzed in Figure 3, the resulting image resolution was typically 5 μm using the singlet lens designed for 1 μm focusing of a 355 nm UV laser. As for the imaging resolution, the treatment of matrix solution also draws certain limitations on MALDI mass spectrometric imaging. The matrix solution that extracts analytes from the sample surfaces also allows diffusion of the analytes within the solution while drying to co-crystallization. Along with irregularity of resulting matrix crystals, it

results in an inherent resolution limit more than 10 μm in the mass images. Thus, the present 5 μm resolution of the developed imaging instrument offers the best instrumental specification practically required for MALDI mass spectrometric imaging.

Conclusions

Here we reported the construction of a MALDI imaging mass spectrometer that achieves mass spectrometric imaging with a high-lateral resolution of about 5 μm . For the high-lateral resolution imaging mass spectrometry, we developed a singlet, aspheric lens with a diameter of 40 mm that was successfully implemented into the ion source of a TOF mass spectrometer. As it uses only a single lens for laser focusing, it provides a more compact design than the previous bulky objective lens assembly of 90 mm O.D. containing 5 lenses with diameters of 30 mm to 50 mm.¹² The compact design may facilitate its application for broad mass spectrometry platforms, providing better sensitivity with a shorter assembly length while still offering high-lateral resolution for imaging. This imaging mass spectrometer will serve biological investigations and bioclinical applications by providing with its high-lateral resolution, biochemical information-rich images in a label-free way, and it also opens opportunities for unbiased investigations.

Acknowledgments. This work was supported by the Biosignal Analysis Technology Innovation Program (2012-0006053) of MEST via KOSEF.

References

1. McDonnell, L. A.; Heeren, R. M. A. *Mass Spectrom. Rev.* **2007**, *26*, 606.
2. Schwamborn, K.; Caprioli, R. M. *Nat. Rev.* **2010**, *10*, 639.
3. Vegvari, A.; Fehniger, T. E.; Gustavsson, L.; Nilsson, A.; Andren, P. E.; Kenne, K.; Nilsson, J.; Laurell, T.; Marko-Varga, G. *J. Proteom.* **2010**, *73*, 1270.
4. Seeley, E. H.; Oppenheimer, S. R.; Mi, D.; Chaurand, P.; Caprioli, R. M. *J. Am. Soc. Mass Spectrom.* **2008**, *19*, 1069.
5. Astigarraga, E.; Barreda-Gomez, G.; Lombardero, L.; Fresnedo, O.; Castano, F.; Giral, M. T.; Ochoa, B.; Rodriguez-Puertas, R.; Fernandez, J. A. *Anal. Chem.* **2008**, *80*, 9105.
6. Kim, J.; Han, S.-P.; Kim, J.; Kim, Y.-J. *Bull. Korean Chem. Soc.* **2011**, *32*, 915.
7. Groseclose, M. R.; Andersson, M.; Hardesty, W. M.; Caprioli, R. M. *J. Mass Spectrom.* **2007**, *42*, 254.
8. Stauber, J.; MacAleese, L.; Franck, J.; Claude, E.; Snel, M.; Kaletas, B. K.; Wiel, I. M. V. D.; Wisztorski, M.; Fournier, I.; Heerena, R. M. A. *J. Am. Soc. Mass Spectrom.* **2010**, *21*, 338.
9. Ha, N. Y.; Kim, S. H.; Lee, T. G.; Han, S. Y. *Langmuir* **2011**, *27*, 10098.
10. Kang, H. S.; Lee, S. C.; Park, Y. S.; Jeon, Y. E.; Lee, J. H.; J, S.-Y.; Park, I. H.; Jang, S. H.; Park, H. M.; Yoo, C. W.; Park, S. H.; Han, S. Y.; Kim, K. P.; Kim, Y. H.; Ro, J.; Kim, H. K. *BMC Cancer* **2011**, *11*, 465.
11. Franck, J.; Arafah, K.; Elayed, M.; Bonnel, D.; Vergara, D.; Jacquet, A.; Vinatier, D.; Wisztorski, M.; Day, R.; Fournier, I.; Salz, M. *Mol. Cell. Proteomics* **2009**, *8*, 2023.
12. Bateson, H.; Saleem, S.; Loadman, P. M.; Sutton, C. W. *J. Pharmacol. Toxicol. Methods* **2011**, *64*, 197.
13. Wiley, W. C.; McLaren, I. H. *Rev. Sci. Instrum.* **1955**, *26*, 1150.
14. Spengler, B.; Hubert, M. *J. Am. Soc. Mass Spectrom.* **2002**, *13*, 735.
15. Chaurand, P.; Schriver, K. E.; Caprioli, R. M. *J. Mass Spectrom.* **2007**, *42*, 476.
16. Koestler, M.; Kirsch, D.; Hester, A.; Leisner, A.; Guenther, S.; Spengler, B. *Rapid Commun. Mass Spectrom.* **2008**, *22*, 3275.
17. Rompp, A.; Guenther, S.; Schober, Y.; Schulz, O.; Takats, Z.; Kummer, W.; Spengler, B. *Angew. Chem. Int. Ed.* **2010**, *49*, 3834.
18. Luxembourg, S. L.; Mize, T. H.; McDonnell, L. A.; Heeren, R. M. *Anal. Chem.* **2004**, *76*, 5339.
19. Jungmann, J. H.; MacAleese, L.; Buijs, R.; Giskes, F.; de Snaijer, A.; Visser, J.; Visschers, J.; Vrakking, M. J.; Heeren, R. M. *J. Am. Soc. Mass Spectrom.* **2010**, *21*, 2023.
20. Moon, J. H.; Yoon, S. H.; Kim, M. S. *Bull. Korean Chem. Soc.* **2005**, *26*, 763.